

# Predicting Human Thermal Comfort in Automobiles

John P. Rugh and Desikan Bharathan  
National Renewable Energy Laboratory

Copyright © 2005 SAE International

## ABSTRACT

The National Renewable Energy Laboratory (NREL) has developed a suite of thermal comfort tools to help develop smaller and more efficient climate control systems in automobiles. The tools consist of a thermal comfort manikin, physiological model, and psychological model that are linked together to assess comfort in a transient non-homogeneous environment. The manikin, which consists of 120 individually controlled zones, mimics the human body by heating, sweating, and breathing. The physiological model is a 40,000-node numerical simulation of the human body. The model receives heat loss data from the manikin and predicts the human physiological response and skin temperatures. Based on human subject test data, the psychological model takes the temperatures of the human and predicts thermal sensation and comfort. The manikin and models have been validated against physiological data that are available in the literature and test subject data that are used to develop the psychological model. This paper presents details on NREL's thermal comfort tools and the validation testing performed.

## INTRODUCTION

Almost all vehicles sold today in Europe, Japan, and the United States have air conditioning (A/C). A/C has become a near-standard feature on new vehicles because it provides driving comfort and reduced road noise and improves safety by rapidly demisting windows and enhancing driver vigilance.

An operating A/C system compressor is the largest ancillary load on an automobile (the alternator load is typically second and hydraulic power steering is third). An A/C compressor can add 5-6 kW of peak power draw on a vehicle's engine, which is about the same as an A/C load in a small single-family home. This load significantly affects the fuel economy of traditional vehicles. The impact on advanced vehicles such as electric, hybrid electric, and fuel cell vehicles is even greater. An NREL study<sup>1</sup> showed that the United States uses 7 billion gal (26.4 billion L) of fuel per year for light-duty vehicle A/C, equivalent to 5.5% of the total national

light-duty vehicle fuel use and 9.5% of the imported crude. The fuel use percentages are based on a total annual light-duty vehicle fuel use of 125.9 billion gal (477 billion L)<sup>2</sup> and imported oil of 73 billion gal (276 billion L)<sup>3</sup>.

Our goal at NREL is to help the automotive industry reduce the fuel used for A/C. NREL is investigating techniques to reduce the peak soak temperature, which allows the A/C system size to be reduced. We are also looking at improved delivery systems and alternative methods to cool the passenger compartment, which will reduce the power requirements of a climate control system.

Since a key requirement is to maintain or enhance passenger comfort, we need to understand how advanced cooling techniques will affect human thermal comfort. NREL has developed a portfolio of thermal comfort tools, including an ADvanced Automotive Manikin (ADAM), Human Thermal Physiological Model, and Human Thermal Comfort Empirical Model to assess comfort in automobile passenger compartments<sup>4</sup>.

Commonly used models for assessing automotive passenger comfort are based on steady-state uniform environment data. Accurately modeling human heat loss in a transient, non-uniform thermal environment is difficult. Factors that contribute to the complexity include:

- Thermal radiation view factors
- Heat transfer between clothing layers
- Thermal and moisture capacitance of clothing
- Clothing to skin contact area
- Clothing to skin thermal resistance
- Clothing fit, including microvolumes
- Non-uniform thermal properties of clothing ensembles
- Non-uniform, transient velocity field around the body
- Modeling evaporation of sweat.

We are including these effects to take automotive passenger comfort assessment to the next level.

## THERMAL COMFORT TOOLS

### OVERVIEW

The integrated system consists of the thermal manikin and the finite element physiological model of the human body. The manikin provides a simulated body positioned in a complex transient thermal environment with multiple heat transfer modes: thermal radiation, natural and forced convection, conduction, and evaporation. The finite element model provides the manikin with a control algorithm that represents human thermal response. A third computational tool predicts local and global transient thermal sensation and comfort.

The thermal manikin (Figure 1) is essentially a surface sensor that measures the rate of heat loss at 120 independently controlled zones. The skin heat transfer rates are sent to the physiological model, which computes the skin and internal temperature distribution and surface sweat rates. This information is then sent back to the manikin, which generates the prescribed skin temperatures, surface sweat rates, and breathing rates. This loop continues to provide a transient measurement tool. The psychological comfort model uses temperature data from the physiological model to predict the local and global thermal comfort as a function of local skin and core temperatures and their rates of change. Using this manikin as a sensor integrates the complex clothing and environmental heat exchange factors into local heat loss measurements from the skin surface.



**Figure 1. ADAM, the Advanced Automotive Manikin**

The physiological model can regulate the manikin for human-realistic spatial and temporal thermal response. The manikin can also be controlled with traditional regulation methods: constant skin temperature or constant heat flux that corresponds to metabolic activity level. Setpoints are individually adjustable for each zone controller. Surface sweating rates can be specified separately for each zone.

The manikin is sized to match the dimensions of a 50<sup>th</sup> percentile western person, the average of the average male and female. Currently the model is sized to match the manikin, but it could be parametrically adjusted to a larger or smaller body. The manikin is a fixed size, but the heat flux ( $W/m^2$ ) is reported to the model; therefore, the heat transfer will scale with model body size.

### ADVANCED AUTOMOTIVE MANIKIN

ADAM is a sophisticated surface sensor that interacts with his environment<sup>5</sup>. He responds to thermal inputs such as radiation and convection and affects the environmental flow and temperature fields. He was designed with the following general capabilities and characteristics:

- Detailed spatial and rapid temporal control of surface heat output and sweating rate
- Surface temperature response time that approximates human skin
- Realistic and uniform sweating
- Human-like geometry and weight with prosthetic joints to simulate the human range of motion
- Breathing with inflow of ambient air and outflow of warm, humid air at realistic human respiration rates
- Complete self-containment, including battery power, wireless data transfer, and internal sweat reservoir for at least 2 h of use with no external connections
- Rugged, durable, low-maintenance construction.

The manikin is approximately 175 cm tall. A Non-Uniform Rational B-Splines digital model of the human body was reshaped in CAD to comply with the 50<sup>th</sup> percentile target and allows the manikin to be manufactured with digital methods. He weighs approximately 61 kg. Although he weighs less than an average male, he is heavy enough to compress the seat and give a realistic contact area.

The manikin's fundamental components are the 126 individual surface segments, each with a typical surface area of 120 cm<sup>2</sup>. Each segment (Figure 2) is a stand-alone device with integrated heating, temperature sensing, sweat distribution and dispensing, heat flux gauge, and a local controller to manage the closed-loop operation of the zone. The high thermal conductivity of the all-metal construction of the sweating surface yields increased thermal uniformity and response speed. A high porosity layer within the surface provides lateral sweat distribution while the lower porosity exterior promotes uniform sweat across the surface. Distributed resistance wire provides uniform heating across the zone surface. Six segments are controlled in pairs, and result in 120 separately controlled zones. A single zone controller, including flow control, is mounted directly on the back of each segment. The zone heat flux gauge measures heat loss into the manikin interior from that zone.

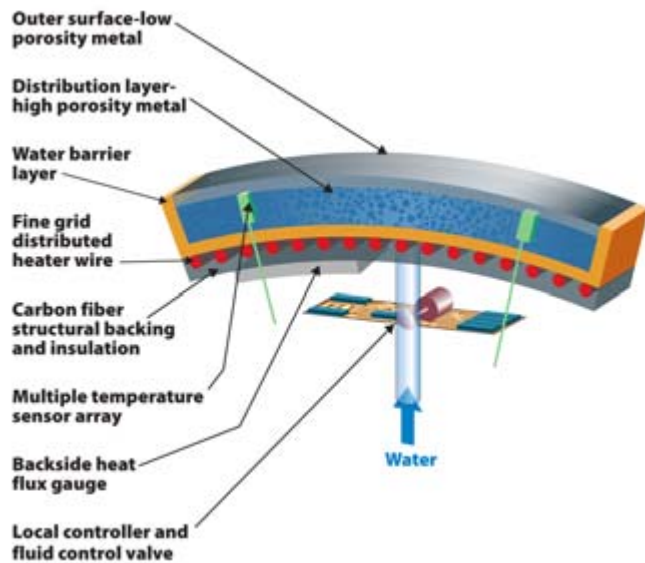


**Figure 2. Manikin Segment**

The manikin's skeleton is composed of laminated carbon fiber, which supports its structure, houses all internal components, and provides mounting locations for surface zones. The joints connect the skeleton parts to give the manikin a human-like form. The adjustable friction joints are pre-tensioned so it can be posed in specific human positions. The wiring harness and sweat tubes pass through the joints.

The manikin needs no external cabling. It uses the internal battery power pack (four internal NiMH battery modules in the torso and thighs) and a wireless communication system that transfers data via 802.11b WiFi communication protocol. For applications that do not require wireless operation, the system can be plugged into an external power supply and communication port for continuous operation and battery charging.

The surface emissivity of 0.5 is lower than typical skin emissivity of 0.95. Since the radiation heat transfer for segments covered by clothing is low, the impact of the difference in emissivities is negligible. We are monitoring unclothed segments (head, hands) and we may have to reduce the heat loss reported to the model for these segments.

When the manikin is standing, two lower back and two kneecap zones recess into its interior compared with a sitting position. The physiological model accounts for active and inactive zones, depending on the manikin's posture.

The skin temperature of each zone is determined by an array of thermistors (typically four) on each zone. A heat flux gauge integrated onto the internal surface of each zone measures heat transfer between the surface zones and the internal body cavity.

We performed a heat balance according to Equation 1 to determine the heat loss from the segment exterior surface.

$$Q_{\text{loss}} = Q_{\text{gen}} - Q_{\text{interior}} - Q_{\text{stored}} \quad (1)$$

Where

$Q_{\text{gen}}$  = electrical heat generation

$Q_{\text{interior}}$  = heat transfer to the interior of the manikin

$Q_{\text{stored}}$  = change in internal energy

The manikin affects the moisture level in the passenger compartment by sweating and breathing. The breathing system permits inhalation and exhalation rates of up to 4 L/min. The breathing system can also permit continuous high levels of exhalation at 8 L/min.

ADAM was built by Measurement Technology Northwest (MTNW) in Seattle, Washington. The characteristics that make ADAM a unique thermal manikin are:

- High spatial resolution (120 zones)
- Self-contained
- Uniform sweating and heating over the entire area of the manikin
- Finite element physiological model control.

#### HUMAN THERMAL PHYSIOLOGICAL MODEL

The NREL Human Thermal Physiological Model is a three-dimensional transient finite element model of the human body. The model simulates the human internal thermal physiological systems such as muscle and blood, and thermoregulatory responses such as metabolic heat generation. The model was developed with the commercially available finite element software ANSYS. This software computes heat flow by conduction, convection, and mass transport of the blood. A human tissue system represents the human body, including the physiological and thermal properties of the tissues. The arms and legs consist of bone, muscle, fat, and skin. There are additional lung and abdominal tissues in the torso and brain tissues in the head. The model calculates the conduction heat transfer based on the temperature gradients between the tissue nodes. The mesh is shown in Figure 3.

Blood flow is modeled with a network of supply and return pipe elements within each body zone (Figure 4). The diameter of the pipes decreases from the center of each zone outward, toward the skin and extremities. The flow in the pipes is modeled as Poiseuille flow, and the convection heat transfer and temperature are solved at each node in the pipe network.



**Figure 3. Human Body Mesh**

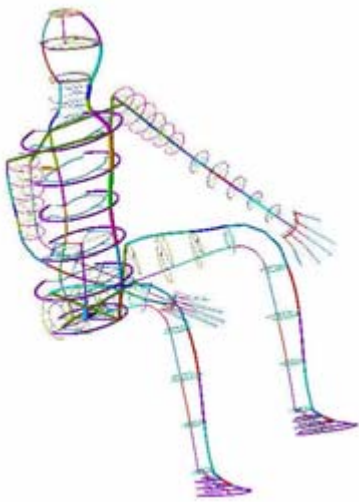


**Figure 4. Circulatory System**

The physiological model was generated in sections with ANSYS. The sections consist of hand, lower arm, upper arm, foot, lower leg, and thigh, one each for the left and right sides. The body was developed as a torso together with neck and head. Each part was generated individually and populated with arteries and veins. The primary blood vessels join via capillaries that are adjacent to the skin layer. The blood vessel diameters were sized to allow blood to flow to each body part at an overall nominal pressure difference of 70 mmHg between the blood supply and return. The tissues were modeled with ANSYS Solid70 elements, and the blood flow pipes use Fluid116 elements. Tissue properties were taken from tables provided by Gordon et al<sup>6</sup> (Table 1). The overall masses and mass distribution for each part in the model compare favorably to those of a human. Deviations are nominally less than 5%.

Each body part is connected to its adjacent part with veins and arteries. In the limbs, the tissues are not connected between parts. In the torso, which is modeled as an integral part, all tissues are connected. An additional pipe network to simulate airflow through the trachea and lungs is included in the torso.

The thermoregulatory system controls physiological responses, such as vasomotor control, sweating, shivering, and metabolic changes.

**Table 1. Thermal Properties of the Human Body**

Tissue or Fluid	Thermal Conductivity (W/m-K)	Density (g/cm <sup>3</sup> )	Specific Heat (J/g-K)
Brain	0.53	1.05	3.69
Abdomen	0.55	1.05	3.69
Lung	0.28	0.55	3.71
Bone (leg)	2.28	1.7	1.59
Muscle	0.42	1.05	3.77
Fat	0.16	0.85	2.51
Skin	0.21	1.0	3.77
Blood	0.52	1.06	4.0

The vasoconstriction/dilation response varies with skin and core temperatures, and with each body zone. The diameters of the pipes in the skin layer can constrict or dilate. The equations that control vasoconstriction/dilation are based on medical experiments<sup>7</sup>.

The sweating response is a function of skin and core temperatures and the number of sweat glands in each zone. The degree of shivering depends on skin and core temperatures and the amount of muscle in each zone. The cardiac output or flow through the pipe network is a function of the metabolic rate and skin and core temperatures<sup>7</sup>.

Given a set of heat flux boundary conditions on the skin, the model currently requires about 2 min to converge at a temperature distribution. We expect to reduce this time to 1 min by streamlining the model and eliminating the large amount of input/output that occurs during a normal ANSYS run.

In principle, the physiological model can operate independently of the manikin. A computational fluid dynamics (CFD) model of a passenger compartment could provide the human skin heat transfer data to the model. However, detailed knowledge of the transient, non-uniform, thermal environment is required. For example, all the view factors for thermal radiation must be calculated, local evaporation rates determined, clothing properties (including fit, thermal resistance, thermal and moisture capacitance, and microvolumes) specified, and a detailed transient flow field calculated.

#### HUMAN THERMAL COMFORT EMPIRICAL MODEL

The University of California, Berkeley (UCB) performed 109 human subject tests (Figure 5) in its Controlled Environmental Chamber under a range of steady-state and transient thermal conditions to explore the relationship between local thermal conditions and perception of local and overall thermal comfort. Core

and local skin temperature data and subjective thermal perception data were obtained via a simple form. These data were used to develop a predictive model of thermal comfort perception<sup>8</sup>. Details of the subject testing and analysis are available in Zhang<sup>9</sup>.

The subject sample size was somewhat limited, and did not include a wide variety of ages, weights, and body compositions. Table 2 shows the characteristics of the 27 subjects.



Figure 5. Thermal Comfort Human Subject Testing

## VALIDATION TESTING

Initial testing was performed to verify the manikin was functioning properly. The first test was a nude manikin test to measure the nude thermal resistance and compare the results to other thermal manikins manufactured by MTNW. Two tests were performed in a climate control chamber at MTNW and the results were averaged. ADAM was configured in a standing position. The room air temperature was maintained at 20°C and 23°C for the 2 tests and manikin skin temperature was set to 34°C with no sweat. Equation 2 was used to calculate the heat transfer resistance.

$$R_a = \frac{T_{s,n} - T_o}{Q_a} \quad (\text{m}^2 \text{ } ^\circ\text{C/W}) \quad (2)$$

where

$T_{s,n}$  = skin temperature

$T_o$  = air temperature

$Q_a$  = heat loss from the manikin

Figure 6 shows that ADAM's nude thermal resistance compares well with the other manikins.

Table 2. Subject Information from the UCB Testing

ID	Gender	Age	Height (cm)	Weight (kg)	Body fat (%)
1	F	43	161	55.6	24
2	F	27	160	51.2	20
3	F	40	173	55.2	17
4	M	20	173	70.0	17
5	M	43	180	72.0	13
6	F	25	165	77.2	41
7	F	24	149	49.8	19
8	M	27	172	67.0	16
9	F	47	166	78.0	39
10	M	29	174	68.4	16
11	F	21	162	72.0	40
12	F	21	169	65.0	28
13	F	21	164	59.0	29
14	F	42	153	60.0	49
15	F	24	167	77.0	33
16	M	34	173	75.8	19
17	F	24	176	71.2	29
18	M	40	179	81.2	19
19	F	25	155	58.4	26
20	M	28	173	69.0	20
21	F	29	174	81.4	41
22	M	37	170	70.0	22
23	M	30	177	75.8	23
24	M	51	181	80.0	17
25	M	33	169	68.0	20
26	M	40	170	68.5	20
27	F	34	163	47.5	17

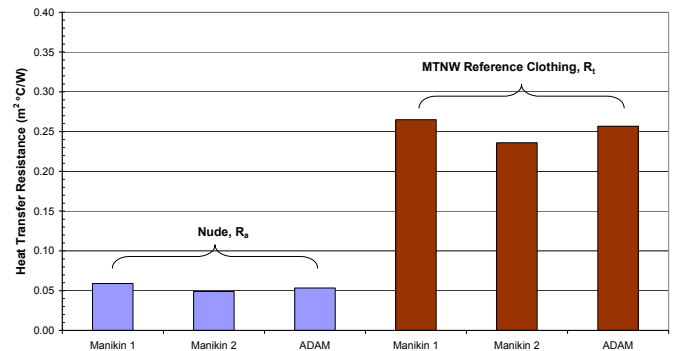


Figure 6. Nude and Total Thermal Resistance of MTNW Manikins and ADAM

We also performed tests with MTNW's reference clothing ensemble (Figure 7). As with the nude tests, the manikin skin temperature was maintained dry at 34°C and the chamber air temperature at 20°C. We used Equation 3 to calculate the total thermal resistance.

$$R_t = \frac{T_{s,cl} - T_o}{Q_{cl}} \quad (\text{m}^2 \text{ } ^\circ\text{C/W}) \quad (3)$$

The total thermal resistance also compared favorably to the data from previously tested manikins (Figure 6). This gives us confidence that the heat loss measured by the manikin segments is accurate.



**Figure 7. MTNW Reference Clothing Test**

After ADAM was delivered to NREL, we continued the validation testing. We ran a series of tests to compare ADAM's skin temperatures to steady-state data from Werner and Reents<sup>10</sup>. We placed ADAM nude and horizontal in our Manikin Climate Control Chamber. The room was maintained at a uniform temperature with negligible air flow. We ran ADAM with physiological model control. Although the actual metabolic rates of the subjects are unknown, the suggested  $45 \text{ W/m}^2$  for a reclining human from the *ASHRAE Fundamentals Handbook*<sup>11</sup> was applied to the human in the model.

We compared the resulting core and skin temperatures to the Werner and Reents data in Figure 8 for an air temperature of  $23.2^\circ\text{C}$ . The manikin/model tended to predict warmer skin temperatures than those measured with a maximum deviation of  $4.2^\circ\text{C}$ . The overall trends were encouraging: the core temperature compared within  $0.6^\circ\text{C}$  and skin temperatures decreased in regions further from the torso (Figure 9).

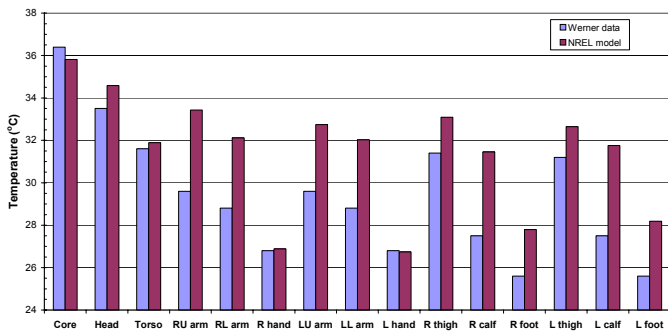


**Figure 8. Comparison of ADAM with Human Data,  $T_{\text{air}}=23.2^\circ\text{C}$**

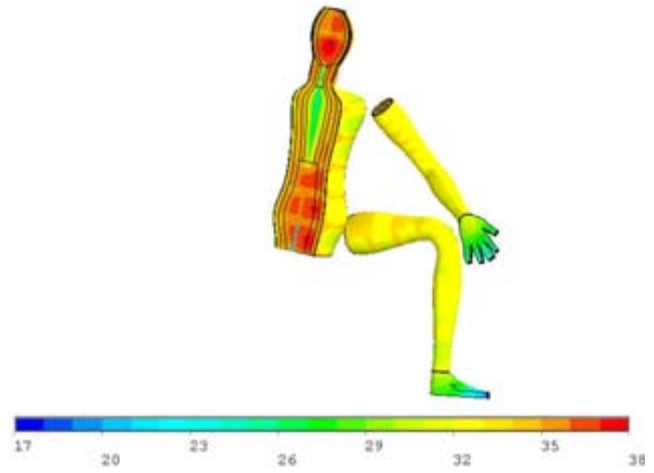


**Figure 9. Temperature Contour Plot - Cross Section**

Figure 10 shows the comparison for an air temperature of  $30^\circ\text{C}$ . The core temperature was within  $0.1^\circ\text{C}$  and the maximum skin temperature deviation was  $2.1^\circ\text{C}$  at the hands. Figure 11 shows that the manikin and model underpredict skin temperatures at higher ambient air temperatures. The core temperature matched exactly, but the maximum underprediction was  $2.5^\circ\text{C}$  at the hands.

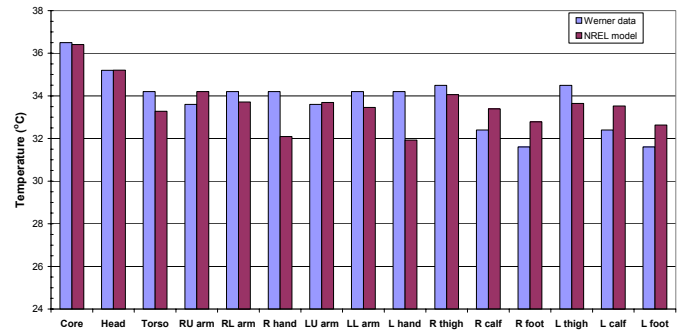


**Figure 10. Comparison of ADAM with Human Data,  $T_{\text{air}}=30^\circ\text{C}$**

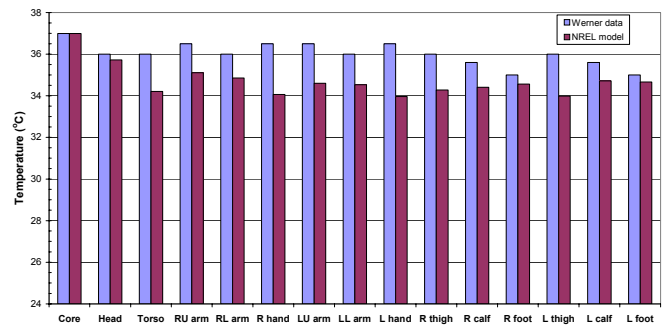


**Figure 11. Comparison of ADAM with Human Data,  $T_{\text{air}}=38^\circ\text{C}$**

Overall the model predicted the core temperature well, which is important because the physiological responses are strong functions of core temperature. The skin temperatures showed slight deviation. We do not know exactly where the temperatures were measured or the uncertainty, so drawing conclusions is difficult. We decided to continue validation testing to compare to measured thermal sensations and comforts, our primary objective.

UCB provided temperature, sensation, and comfort data from a human subject for a steady-state uniform environment test. The exact locations of the temperature measurements were identified so we could select segments on ADAM for comparison. We matched the environmental conditions in our Manikin Climate Control Chamber. The average air temperature was 28.6°C and the relative humidity was 35%. ADAM was configured standing, as seen in Figure 12. Since the UCB human subject wore a leotard and used an automobile driving simulator during the test, ADAM was dressed in a similar leotard and the metabolic rate was set to 69.8 W/m<sup>2</sup> to correspond to a person driving a vehicle.

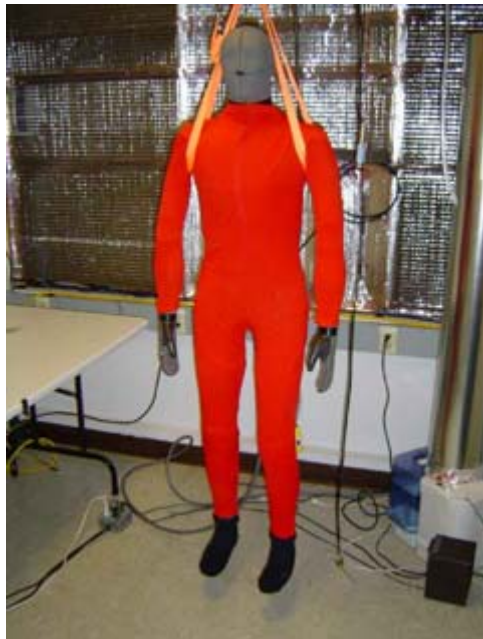
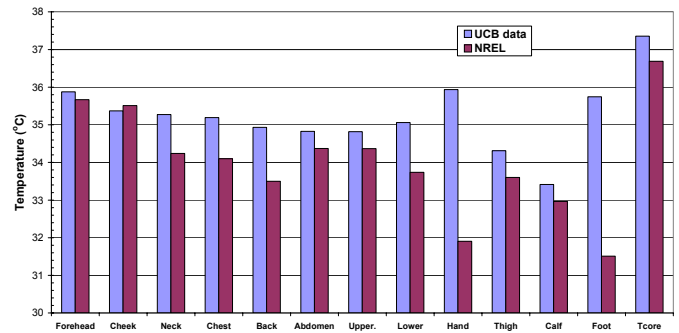


**Figure 12. ADAM wearing the UCB Leotard**

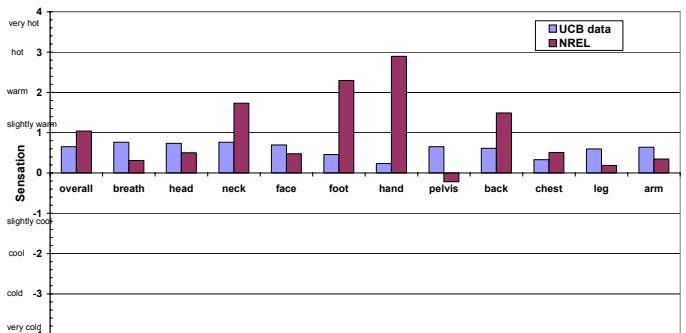
Figure 13 shows the skin temperatures matched the human data well, although the predicted hand and foot temperatures were low. Since the predicted hand and foot temperatures were within 2°C of the measured Werner data, the difference observed here could be due to the physiology of the human subject or the measurement uncertainty. Excluding the hands and feet, the skin temperatures matched within 1.4°C and the core temperature was within 0.7°C.

Figure 14 shows the measured and predicted sensations. The environment is close to neutral as defined by Fanger<sup>12</sup> and the sensations reflect this, being close to zero. The predicted sensations matched

the data fairly well, although the hand and foot sensations were significantly off because of the low skin temperature. Excluding the hands and feet, the predicted sensations matched the human data within 1.0.



**Figure 13. Predicted Skin Temperatures Compared to UCB Subject Data, T<sub>air</sub>=28.6°C**



**Figure 14. Predicted Thermal Sensation Compared to UCB Subject Data, T<sub>air</sub>=28.6°C**

Figure 15 shows the predicted thermal comfort compared to the UCB human data. The predicted overall comfort was within 0.3 of the measured value. We are reviewing human subject data to determine whether a weighted average of the local comforts will yield better predictions of overall thermal comfort for off-neutral conditions. Figure 15 shows a straight average compared to the current psychological overall comfort correlation and the measured overall comfort. Although the measured local comforts were close to neutral, the predicted local comforts showed some variation. It should be noted that this is a comparison with a single individual, so person-to-person variations could be responsible for some of the differences.

ADAM is almost ready for vehicle testing. One area that requires further investigation is the response time of the manikin/physiological model system. We will perform a whole body step change test that will involve moving ADAM from one environment outside the chamber to the chamber and back again. UCB ran this test and provided human data for comparison.

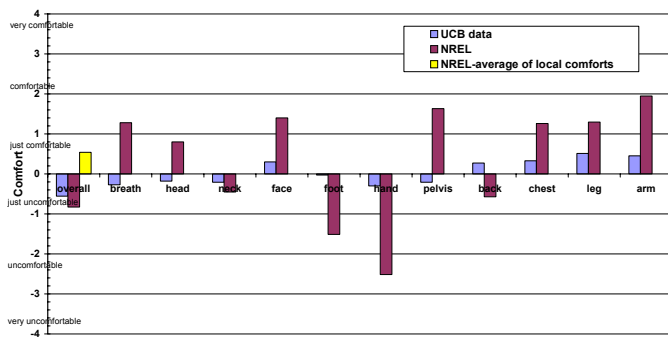


**Figure 15. Predicted Thermal Comfort Compared to UCB Subject Data, T<sub>air</sub>=28.6°C**

Another area that requires further research is repeatability. Once we verify consistent results run-to-run, the advantage of using a manikin for sensation and comfort assessment will be realized. Although technical glitches can occur, the manikin will not experience the human variations (mood swings, time since last meal, etc.) that affect the assessment of comfort. The new thermal comfort tools permit detailed, repeatable measurement and evaluation of human thermal comfort.

## CONCLUSION

NREL has developed a suite of thermal comfort tools to assess human thermal comfort in automobiles. These tools include ADAM, a Human Thermal Physiological Model, and a Human Thermal Comfort Empirical Model. Our objective is to use these tools to optimize thermal comfort while reducing A/C fuel use.

Validation testing of the manikin/model is ongoing. Testing at MTNW shows the heat loss from ADAM matches heat losses from other similar manikins. The total resistance of MTNW's calibration clothing measured by ADAM also compared closely with measurements from other manikins.

Initial results indicate the manikin with physiological model control yields human-like skin temperature distribution. Compared to data from Werner, the skin temperatures were within approximately +4.2/-2.5°C for a wide range of ambient air temperatures. The core temperatures matched within 0.6°C.

Comparison with subject data from UCB also shows the predicted skin temperature distribution of the manikin and model is similar to that of the human subject except for the hand and foot. Since the hand and foot skin temperatures had less deviation compared to the Werner data, the physiology of the UCB subject may be responsible for the differences. Excluding the hands and feet, the skin temperatures were within 1.4°C and the core temperature was within 0.7°C in a uniform environment of 28.6°C. The predicted overall thermal sensations and comforts match the human data well and

give us confidence to continue validation testing, which includes simulating a whole body step change. The next step is to test vehicle A/C systems.

## ACKNOWLEDGMENTS

The authors gratefully acknowledge the support of the U.S. Department of Energy in developing, fabricating, and testing the thermal manikin and physiological model. DOE's Office of FreedomCAR and Vehicle Technologies (OFCVT) supported this work. The authors appreciate the support of Roland Gravel, DOE Program Manager; Terry Penney, NREL's OFCVT Technology Manager; and Barbara Goodman, Director of the Center for Transportation Technologies and Systems. Rob Farrington, NREL Advanced Vehicle Systems Group Manager, was instrumental in the development of the thermal comfort tools.

The authors would also like to thank Rick Burke and Steve Rodriguez at Measurement Technology Northwest, Hui Zhang and Charlie Huizenga at the University of California Berkeley, and Andreas Valahinos at Advanced Engineering Solutions.

## REFERENCES

1. Rugh, J.; Hovland, V.; and Andersen, S. (2004) Significant Fuel Savings and Emission Reductions by Improving Vehicle Air Conditioning, Mobile Air Conditioning Summit, Washington, D.C., April 14-15, 2004.
2. Wards 2001 Automotive Yearbook.
3. U.S. Department of Energy's Energy Information Administration, April 2001, <http://www.iea.doe.gov/cabs/usa.html>.
4. McGuffin, R. and Burke, R. "Modeling of Human Thermal Comfort," Proceedings of the 5th Vehicle Thermal Management Systems Conference, SAE 2001-01-1739, Nashville, TN. 2001.
5. Burke, R.; Rugh, J.; and Farrington R. (2003) ADAM – the Advanced Automotive Manikin, 5th International Meeting on Thermal Manikins and Modeling, Strasbourg, France.
6. Gordon, R. G.; Roemer, R. B.; and Horvath, S. M. (1976) A Mathematical Model of the Human Temperature Regulatory System – Transient Cold Exposure Response. IEEE Transactions on Biomedical Engineering 23, no. 6: 434-444.
7. Smith, C. E. (1991) A Transient, Three-Dimensional Model of the Human Thermal System. Ph.D. Thesis, Kansas State University.
8. Zhang, H.; Huizenga, C.; Arens E.; and Wang, D. (2004) Thermal Sensation and Comfort in Transient Non-Uniform Thermal Environments, European Journal of Applied Physiology, Vol. 92, Number 6, Pages 728-733, September 2004.
9. Zhang, H. (2004) Human Thermal Sensation and Comfort in Transient and Non-Uniform Thermal Environments, Ph.D. Thesis, U.C. Berkeley.

10. Werner, J. and Reents, T. (1980) A Contribution to the Topography of Temperature Regulation in Man, European Journal of Applied Physiology, 1980, 45:87-94.
11. 2001 ASHRAE Fundamentals Handbook, Page 8.7.
12. Fanger, P. O. (1970) Thermal Comfort, Analysis and Applications in Environmental Engineering, McGraw-Hill.

## **CONTACTS**

john\_rugh@nrel.gov

desikan\_bharathan@nrel.gov

<http://www.ott.doe.gov/coolcar>